Theoretical DFT Study of Fragmentation and Association of Heme and Hemin†

O. P. Charkin*

Institute of Problems of Chemical Physics, Russian Academy of Sciences, Institutskii prosp. 18, Chernogolovka, Moscow Region, 142432 Russia

N. M. Klimenko

Lomonosov State Academy of Fine Chemical Technology, Vernadskii prosp. 86, Moscow, 117571 Russia

D. O. Charkin

Chemical Department, Moscow State University, Vorob'evy gory, Moscow, 119992 Russia

H.-C. Chang and S.-H. Lin

Institute of Atomic and Molecular Sciences, Academia Sinica, P. O. Box 23-166 Taipei, Taiwan 106, ROC

Received: March 3, 2007; In Final Form: July 24, 2007

The electronic and geometric structures, energy stability, and normal vibrational frequencies of heme, hemine, and their stepwise fragmentation products (with successive loss of two carboxymethyl, four methyl, and two vinyl peripheral groups) in the states with different multiplicity were calculated using the density functional theory (the B3LYP method) with several basis sets. At the same level, the structure and stability of neutral and positively charged dimers of the ferri- and ferroporphyrines were also computed. The computational results are compared with available experimental data. The trends in the behavior of these properties of heme and hemin are analyzed upon the stepwise fragmentation and association and with a change in the multiplicity and external charge. The structure and energetic stability of complexes of the species with molecular oxygen are discussed.

I. Introduction

Metalloporphyrins (MPs) are constituents of numerous proteins. Their biological functions vary from oxygen storage and transport (hemoglobin, myoglobin) to electron transport (cytochrome oxidase) and energy conversion (chlorophyll).[1] In addition, they exhibit photosensitizing and catalytic properties.[2] Due to the diversity of their functions, MPs remain to be objects in numerous spectroscopic studies mainly carried out in the condensed phase where the chemical behavior and reactivity of MPs are significantly influenced by solvent. To study MPs without solvent, the molecules are transferred from the condensed phase to the gas phase as individual ions using electrospray ionization and mass spectrometrical registration of ions.[3] A comparison of the molecular characteristics of MPs in condensed and isolated states is important for quantifying the effect of the environment on the structure of biologically active groups embedded into more complicated substrates. Inasmuch as experimental studies of similar systems in the free state run into technical problems, quantum chemical calculations of potential energy surfaces (PES) can be especially helpful and informative in this case.

Heme ($FeC_{34}H_{32}O_4N_4$), which enters into the composition of hemoprotein active sites, is responsible for oxygen storage and transport. It consists of a porphyrin ring (below P ring) centered by the Fe atom with two propionate, four methyl, and two vinyl peripheral groups (structure **1** in Figure 1). The geometric and electronic structures, stability, and spectroscopic characteristics of heme, as well as mechanisms of the heme reaction with O_2, CO, NO, CN^-, and related ligands are still the focus of systematic experimental and theoretical studies.

The positive heme ion (hemin$^+$, $FeC_{34}H_{32}O_4N_4^+$) in the free state has been studied experimentally.[4,5] In ref 4, dissociation bond energies of the first and the second carboxymethyl groups have been evaluated as $D_1 \sim 2.4$ eV and $D_2 \ll D_1$, but the electronic and geometric structures of the hemin$^+$ and its degradation products were not addressed. Meanwhile, it is known that the multiplicity of the ground and low-lying states of heme, hemin$^+$, and related species is important for their structure and stability and for elucidating the biological functions of hemoproteins. For example, it was shown[6] that the low-spin complex with the $(d_{xz}d_{yz})^2(d_{xy})^1$ configuration of the metal can play a key role in the processes of heme degradation, while the diversity of reactions catalyzed by cytochrome P450 can be associated with different reactivities of the high- and low-spin states of the oxoiron porphyrin radical cation.[7] The geometric parameters of the iron porphyrins "nuclear Fe@N_4" (R(Fe−N) distances, the displacement h(Fe/NNNN) of the Fe atom along the normal to the NNNN plane) and the ruffled, dome, and other distortions of the P ring can also differ significantly in the states with different spins.[8,9]

In our paper,[5] the hemin$^+$ fragmentation was studied using electrospray mass spectrometry, laser excitation, and the collision-induced dissociation method. Evolution of the hemin$^+$ photofragmentation pattern observed as a function of the laser

† Part of the "Sheng Hsien Lin Festschrift".

* To whom correspondence should be addressed. E-mail: charkin@icp.ac.ru.

10.1021/jp071741q CCC: $37.00
Published on Web 08/30/2007

excitation time (Figure 2) demonstrate that two carboxymethyl groups are the first and most readily removed; the second are the four methyl groups (Figure 3), and finally, the vinyl groups are eliminated, indicating that the energy of their bonds with the P ring increases in the series carboxymethyl $\ll$ methyl $<$ vinyl. The energies of removal of the first and second carboxymethyl groups were measured to be $D_1 \sim 2.4$ and $D_2 \sim 2.9$ eV, in disagreement with the previous evaluation $D_2 \ll D_1$.[4] Knowledge of the precise values of D_1 and D_2 are of principle importance for elucidation of mechanisms of cleavage of the isolated heme and hemin$^+$ from myoglobin.[5]

The present paper is devoted to the DFT study of heme, hemin$^+$, and products of their fragmentation and association in the states of various multiplicity. The paper consists of three parts (following just after the "Computational Details"). In section III, systematical DFT calculations of the electronic and geometric structure, energetic stability, and normal vibrational frequencies are performed for heme, hemin$^+$, and products of their stepwise fragmentation with consecutive loss of two carboxymethyl (CMe) groups from heme and hemin$^+$ and four methyl (Me) and two vinyl (Vi) groups from hemin$^+$

$$FeC_{34}H_{32}O_4N_4\ (\mathbf{1}) \rightarrow FeC_{32}H_{29}O_2N_4\ (\mathbf{2}) + CH_2COOH + D_1{}^0(\mathrm{CMe}) \quad (1)$$

$$FeC_{34}H_{32}O_4N_4{}^+\ (\mathbf{1}) \rightarrow FeC_{32}H_{29}O_2N_4{}^+\ (\mathbf{2}) + CH_2COOH + D_1{}^+(\mathrm{CMe}) \quad (1^+)$$

$$FeC_{32}H_{29}O_2N_4\ (\mathbf{2}) \rightarrow FeC_{30}H_{26}N_4\ (\mathbf{3}) + CH_2COOH + D_2{}^0(\mathrm{CMe}) \quad (2)$$

$$FeC_{32}H_{29}O_2N_4{}^+\ (\mathbf{2}) \rightarrow FeC_{30}H_{26}N_4{}^+\ (\mathbf{3}) + CH_2COOH + D_2{}^+(\mathrm{CMe}) \quad (2^+)$$

$$FeC_{30}H_{26}N_4{}^+\ (\mathbf{3}) \rightarrow FeC_{29}H_{23}N_4{}^+\ (\mathbf{4}) + CH_3 + D_1{}^+(\mathrm{Me}) \quad (3^+)$$

$$FeC_{29}H_{23}N_4{}^+\ (\mathbf{4}) \rightarrow FeC_{28}H_{20}N_4{}^+\ (\mathbf{5}) + CH_3 + D_2{}^+(\mathrm{Me}) \quad (4^+)$$

$$FeC_{28}H_{20}N_4{}^+\ (\mathbf{5}) \rightarrow FeC_{27}H_{17}N_4{}^+\ (\mathbf{6}) + CH_3 + D_3{}^+(\mathrm{Me}) \quad (5^+)$$

$$FeC_{27}H_{17}N_4{}^+\ (\mathbf{6}) \rightarrow FeC_{26}H_{14}N_4{}^+\ (\mathbf{7}) + CH_3 + D_4{}^+(\mathrm{Me}) \quad (6^+)$$

$$FeC_{26}H_{14}N_4{}^+\ (\mathbf{7}) \rightarrow FeC_{24}H_{11}N_4{}^+\ (\mathbf{8}) + C_2H_3 + D_1{}^+(\mathrm{Vi}) \quad (7^+)$$

$$FeC_{24}H_{11}N_4{}^+\ (\mathbf{8}) \rightarrow FeC_{22}H_8N_4{}^+\ (\mathbf{9}) + C_2H_3 + D_2{}^+(\mathrm{Vi}) \quad (8^+)$$

in various spin states (bold figures in brackets correspond to the structures depicted in Figure 1). In addition to determination of the multiplicity and the electronic, structural, and energetic characteristics of the ground states, we were aiming to determine similar properties and relative energies for low-lying excited states with different multiplicities, to evaluate energies of successive loss of the peripheral groups $D_i{}^0$(CMe), $D_i{}^+$(Cme), $D_i{}^+$(Me), and $D_i{}^+$(Vi), and to analyze trends and correlations between multiplicity and the geometric and energetic properties of the species under consideration. With the same goals, in the section IV, the structures and energies for various spin states of the dimer ferriporphyrin $(FeC_{34}H_{31}N_4O_4)_2$, its ion $(FeC_{34}H_{31}N_4O_4)_2{}^+$, and products of their decomposition into corresponding monomers were calculated at the same computational level. In the last sections V and VI, similar calculations were carried out for various spin states of the positively charged and neutral dimers of heme, $(FeC_{34}H_{32}N_4O_4)_2{}^+$ and $(FeC_{34}H_{32}N_4O_4)_2$, and for their complexes with molecular oxygen, correspondingly.

II. Computational Details

In the present paper, all calculations were performed in the framework of the hybrid Becke−Lee−Young−Parr method (B3LYP[8,9]) with several basis sets and using the GAUSSIAN 03 program.[10] The geometry calculated at this level is, as a rule, consistent with the experimental one, and the calculated vibrational frequencies, after an appropriate scaling, reproduce the experimental values better than other computational methods. In this work, optimization of the geometry and calculations of normal vibrational frequencies of heme, hemin$^+$, and their fragments were performed using basis set Gen-1 = 6-31G*-(Fe) + 6-31G(C,H,N,O) with polarization functions on the Fe atom only. Earlier,[5,13] we found that the Gen-1 satisfactory reproduces the geometric parameters and vibrational frequencies of heme and hemin$^+$ calculated with the standard 6-31G* basis set (deviations did not exceed 0.01−0.02 Å, 2−3°, and 15 −30 cm^{-1}, correspondingly) with significant savings of computer time and resources. The same Gen-1 was used for geometry optimization of various multiplets of the ferri- and ferroporphyrin dimers and their complexes with O_2 (vibrational frequencies of the dimers were not calculated due to their complexity). In paragraph III, the total and relative energies of all spin states of the structures **1**−**9** in Figure 1 were refined by single-point calculations with the 6-31G* and 6-311++G** basis sets at the geometry optimized at the B3LYP/Gen-1 level. In paragraphs IV−VI, energetic characteristics of the ferriporphyrin dimers and heme/hemin$^+$ associates were refined with the Gen-2 = 6-311+G*(Fe) + 6-31G* basis set at the geometry optimized at the same B3LYP/Gen-1 level. The spin density ρ on atoms was calculated everywhere with the Gen-1 basis set.

Although B3LYP, to date, is one of the most reliable methods that is used extensively by many authors for calculations of metalloporhyrines both in the ground state and in excited states of various multiplicities (see, for example, refs 11, 12, and 14 and references therein), it should be noted that this method was not calibrated or systematically tested for open-shell systems with various spins. The absolute values of the energy gaps between the multiplets calculated at the B3LYP level can be approximated with a possible error of about a few tenths of an electronvolt.[14] For a set of the close-lying lowest multiplets, the B3LYP method can often be unable to predict definitely which of them is the ground state and which is an excited one. In these cases, the more sophisticated (and much more "expensive") multireference methods are necessary, which are beyond the facilities of our computers. As in our previous papers,[5,13] our attention here was focused mostly on the relative changes (rather then on the absolute values) of the calculated properties and on their trends in various series of heme-related species.

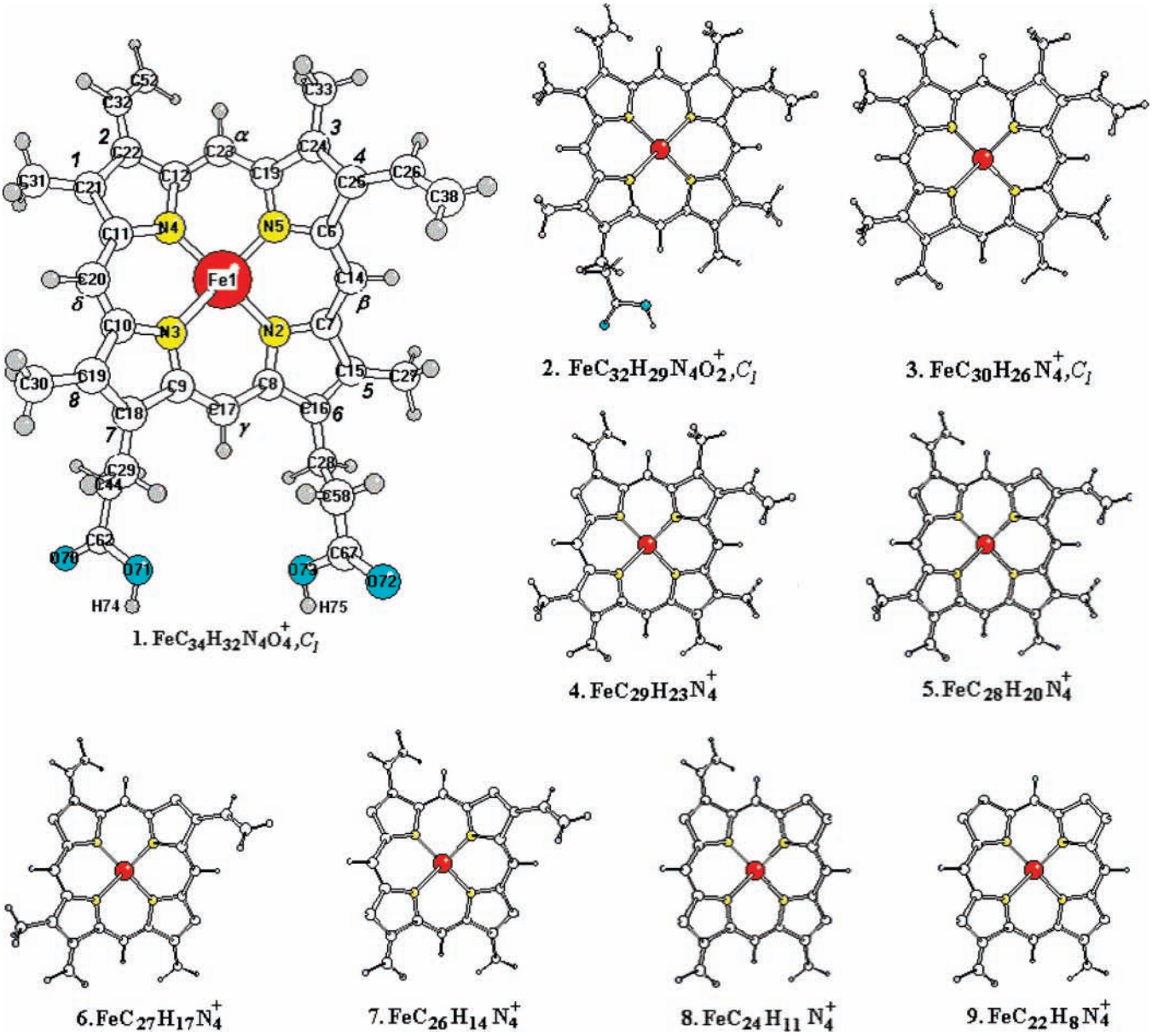

Figure 1. Structures of heme (**1**), either neutral or positively charged, and the fragmentation products (**2**−**9**) after sequential loss of two carboxymethyl, four methyl, and two vinyl groups.

III. Stepwise Fragmentation of Heme and Hemin$^+$ with Consecutive Loss of Peripheral Carboxymethyl, Methyl, and Vinyl Groups

A. Elimination of Carboxymethyl Groups. In accord with our calculations, all optimized structures **1**−**9** (Figure 1) both of the neutrals and of the positive ions in all discussed spin states have all real vibrational frequencies, and each of these states refers to a local minimum of the PES. Table 1 shows that the neutral heme (**1**) molecule has the triplet ground state, in which, as judged from the calculated spin density ρ(Fe) ∼ 2.00 (here and below ρ is given in fractions of *e*), both unpaired electrons are localized at the Fe atom. The nearest quintet with four spins at the Fe atom (ρ(Fe) = 3.74) lies higher only by ∼0.2 eV, whereas the singlet state is less favorable by ∼1.5 eV. This result is qualitatively consistent with the previous experimental and theoretical data on unsubstituted iron porphyrin $FeC_{20}H_{12}N_4$ (D_{4h}),[14,15] which has the triplet ground state, while the quintet lies ∼0.3 eV[14] (or ∼0.7 eV[15]) higher. For the hemin$^+$ ion, the quartet state with three unpaired electrons at Fe (ρ(Fe) ∼2.95) is preferable, while the sextet, in which the Fe atom has four unpaired electrons (ρ(Fe) ∼ 3.86) and one spin delocalized over the P ring, is obviously unfavorable. In the doublet, which is ∼0.5 eV higher than the quartet, Fe has two unpaired electrons (ρ(Fe) ∼ 1.99), and the spin of the P ring is oppositely directed.

For the first neutral product $FeC_{32}H_{29}O_2N_4$ (**2**) with one missing CMe group, the lowest doublet, quartet, and sextet are close in energy within 0.2 eV. In the quartet and sextet states of **2**, one spin is localized at the P ring, while Fe has, respectively, two and four unpaired electrons. The doublet state of neutral product **2** has the spin density distribution similar to that of the doublet of hemin$^+$ (**1**) (Table 1). For the $FeC_{32}H_{29}O_2N_4^+$ (**2**) ion, the triplet and quintet are very close to each other, with all of the unpaired electrons being localized at the metal atom (ρ(Fe) ∼ 1.98 for the triplet and ρ(Fe) ∼3.74 for the quintet).

For the second neutral product $FeC_{30}H_{26}N_4$ (**3**) with two missing CMe groups, the lowest triplet, quintet, and septet are closely spaced within 0.2 eV, and a singlet lies ∼1.5 eV higher. In the triplet and quintet states, the Fe atom has two unpaired

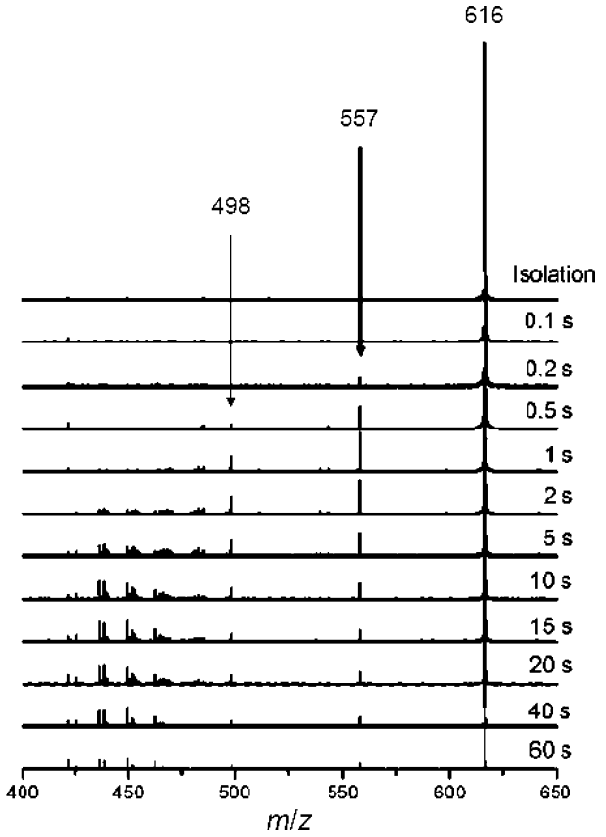

Figure 2. Change of the photofragmentation pattern of isolated hemin$^+$ as a function of laser excitation time. The peaks denoted at m/z 557 and 498 au correspond to [heme$-$$CH_2COOH$]$^+$ and [heme$-$$(CH_2COOH)_2$]$^+$ ions, respectively (see ref 5 for more detail).

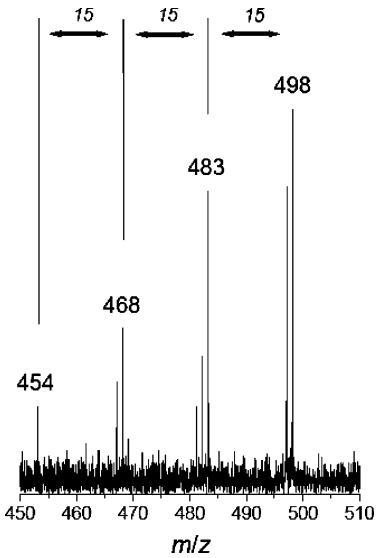

Figure 3. Collision-induced dissociation pattern of the isolated [heme$-$$CH_2COOH$]$^+$ ion ($m/z = 557$ au) with sequential loss of methyl groups ($m/z = 15$ au).[5]

electrons (in both states, ρ(Fe) $\sim$ 2.00) and four spins in the septet (ρ(Fe) $\sim$ 3.75), whereas the P ring retains two spins both in the quintet and septet. For the $FeC_{30}H_{26}N_4^+$ (**3**) ion, the pattern is more complicated; the quartet is preferable, while the doublet and sextet states are, respectively, $\sim$0.6 and $\sim$1.1 eV higher. For the doublet, the spin density distribution is similar to that of the doublet states for hemin$^+$ (**1**) and $FeC_{32}H_{29}O_2N_4$ (**2**). In the sextet, the Fe atom has four unpaired electrons (ρ(Fe) $\sim$ 3.75); in the lowest quartet, one spin is roughly equally distributed between the P ring and the metal atom.

The calculated (according to Mulliken) effective charge Z(Fe) at the metal atom changes in a range from $+0.90$ to $+1.28$ e in all of the systems under consideration, no matter what their external charge and multiplicity.

Table 2 shows that the calculated energies of abstraction of the first and second carboxymethyl groups from hemin$^+$ (**1**), D_1^+(CMe) $\sim$ 1.80 and D_2^+(CMe) $\sim$ 2.40 eV, are in perfect agreement with the experimental values[5] and disprove the conclusion[4] that D_2^+(CMe) is much less than D_1^+(CMe). For degradation of the neutral heme, the calculated energies D_1^0(CMe) and D_2^0(CMe) are on the order of $\sim$2.5$-$2.7 eV. The D_1^0 value is $\sim$0.9 eV higher than D_1^+, whereas D_2^0 and D_2^+ are close to each other.

Analysis of the geometry parameters of heme and hemin$^+$ (these data are collected in refs 5 and 13) show that the lengths of bonds like $C_{29}-C_{34}$ (1.55 Å), $C_{15}-C_{27}$ (1.50 Å), and $C_{25}-C_{26}$ (1.46 Å), which connect the peripheral groups with the P ring, decrease in the order CMe > Me > Vi. The strength of these bonds should increase in the same order, in agreement with the experimentally found sequence of detachment of the peripheral groups from hemin$^+$ (the CMe groups are removed first, the second are the Me groups, and finally, the Vi groups are also eliminated).[5] It should be noted that the calculated average distances R(Fe$-$N) for the triplet (1.995 Å) and quintet (2.058 Å) states of heme (**1**) are close to the corresponding experimental values (1.972 and 2.057 Å, respectively) for the triplet $^3A_{2g}$, Fe(TPP), and quintet $^5A_{1g}$, Fe(TPP)(THF) (TPP is tetraphenylporphyrin; THF is tetrahydrofuran).[16,17]

The distance R(Fe$-$N) is most sensitive to the change in multiplicity; this distance varies within the narrow range of 1.98$-$2.00 Å for low- and intermediate-spin states and increases to 2.05$-$2.07 Å for high-spin states. This tendency, typical of many metalloporphyrins, is related to participation (or nonparticipation) of the $3d_{x^2-y^2}$ Fe AO in the formation of a donor$-$acceptor bond with lone pairs of four nitrogen atoms of the P ring.[15] In the high-spin states, $3d_{x^2-y^2}$, the Fe AO is occupied by an unpaired electron, an efficient donor$-$acceptor interaction is impossible, and the R(Fe$-$N) distance remains large. In the low- and intermediate-spin states of the Fe atom, the $3d_{x^2-y^2}$ Fe AO is vacant and can be involved in the donor$-$acceptor bonding, which is accompanied by a considerable shortening of R(Fe$-$N). As it will be shown below in sections IV, V, and VI, the same picture exists in calculations of the dimers of ferriporphyrin and heme/hemin$^+$ associates.

The calculated vibrational spectra of heme, hemin$^+$, and their fragments are rather complicated.[5,13] We will briefly mention here only those vibrations which are associated with the dominating (or most significant) displacements of the metal atom in the NNNN ring plane (in the range of 270$-$360 cm^{-1}) and normal to this plane (150$-$200 cm^{-1}) and in which the "effect of the $3d_{x^2-y^2}$ Fe AO" is most clearly pronounced. Their analysis shows[5,13] that, for both ranges, the lower values ($\sim$150 and $\sim$270 cm^{-1}) correspond to the high-spin states, and the upper values ($\sim$200 and $\sim$360 cm^{-1}) correspond to the low- and intermediate-spin states, in accord with the shortening and strengthening of the Fe$-$N donor$-$acceptor bonds in the same order.

B. Elimination of Methyl and Vinyl Groups. A search of the ground electronic states of the fragmentation products with missing Me and Vi groups is more a complicated task for several reasons. For example, each of the radicals with the structures of **4**, **5**, or **6** has a set of "positional" isomers corresponding to elimination of the Me or Vi group from different positions of the P ring. Each of the positional isomers has several terms of various multiplicity, and each of these multiplets can correspond

TABLE 1: Relative (E_{rel}) Energies of Electronic States with Various Multiplicities, Effective Charges, and Spin Densities on the Fe Atom in Heme, Hemin$^+$, and the Products of Their Fragmentation with a Sequential Loss of External Groups[a]

species, structure	spin S	E_{rel}[b] eV	Z(Fe) e	ρ(Fe)[c] e	species, structure	spin S	E_{rel}[b] eV	Z(Fe) e	ρ(Fe)[c] e
$FeC_{34}H_{32}N_4O_4$, (**1**)	0	1.45	+0.93		$FeC_{29}H_{23}N_4^+$, (**4**-*5*)	1-*a*	0.0	+0.96	1.97
	1	0.0	+0.99	2.00		2-*a*	0.18	+0.97	2.03
	2	0.17	+1.02	3.74		3-*c*	0.70	+1.28	2.94
$FeC_{34}H_{32}N_4O_4^+$, (**1**)	$^1/_2$	0.51	+0.94	1.99	$FeC_{29}H_{23}N_4^+$, (**4**-*8*)	1-*d*	0.77	+1.18	2.56
	$1^1/_2$	0.0	+1.28	2.95		2-*a*	0.0	+0.95	2.04
	$2^1/_2$	2.01	+1.14	3.86		3-*c*	0.91	+1.27	2.94
$FeC_{32}H_{29}N_4O_2$, (**2**)	$^1/_2$	0.0	+0.91	1.98	$FeC_{28}H_{20}N_4^+$, (**5**)	$1^1/_2$	0.10	+0.96	1.97
	$1^1/_2$	0.07	+0.91	2.00		$2^1/_2$	0.0	+0.96	2.03
	$2^1/_2$	0.20	+1.03	3.75		$3^1/_2$	0.15	+1.08	3.76
$FeC_{32}H_{29}N_4O_2^+$, (**2**)	0	1.57	+1.00		$FeC_{27}H_{17}N_4^+$, (**6**)	1	1.16	+0.98	0.10
	1	0.0	+0.94	1.98		2	0.51	+0.97	1.99
	2	0.19	+1.07	3.74		3	0.0	+1.16	2.47
$FeC_{30}H_{26}N_4$, (**3**)	0	1.45	+0.90		$FeC_{26}H_{14}N_4^+$, (**7**)	$^1/_2$	0.27	+0.98	1.97
	1	0.0	+0.90	1.98		$1^1/_2$	0.53	+0.98	1.98
	2	0.10	+0.92	2.03		$2^1/_2$	0.99	+1.15	2.43
	3	0.22	+1.04	3.75		$3^1/_2$	0.0	+1.16	2.45
$FeC_{30}H_{26}N_4^+$, (**3**)	$^1/_2$	0.58	+0.95	1.95	$FeC_{24}H_{11}N_4^+$, (**8**)	1	0.37	+1.20	1.20
	$1^1/_2$	0.0	+1.16	2.48		2	0.40	+1.16	2.44
	$2^1/_2$	1.10	+1.07	3.75		3	0.0	+0.94	2.01
$FeC_{29}H_{23}N_4^+$, (**4**-*1*)	1-*a*	0.0	+0.96	1.97		4	0.18	+1.16	2.44
	2-*a*	0.21	+0.95	2.02	$FeC_{22}H_8N_4^+$, (**9**)	$1^1/_2$	0.01	+0.98	1.97
	3-*a*	0.36	+1.07	3.75		$2^1/_2$	0.20	+1.00	2.00
$FeC_{29}H_{23}N_4^+$, (**4**-*3*)	1-*a*	0.0	+0.96	1.97		$3^1/_2$	0.0	+1.17	2.46
	2-*a*	0.16	+0.95	2.02					
	2-*b*	1.31	+1.43	0.60					
	3-*c*	0.82	+1.22	2.92					

[a] Calculated at the B3LYP/6-311++G**// B3LYP/Gen-1 + ZPE(B3LYP/Gen-1) level. Bold and italic figures in brackets correspond to the structures depicted in Figure 1 and to the corresponding "positional" isomers (see text). [b] Relative energies of various electronic states with respect to the multiplet with the lowest energy. [c] Spin density on the Fe atom (in units of *e*).

TABLE 2: Dissociation Energies D_i for Sequential Elimination of External Groups from Heme and Hemin$^+$ Calculated at the B3LYP Level with Various Basis Sets (in eV)[a]

(a) Elimination of Carboxymethyl Groups

reaction	Gen-1	6-31G*	6-311++G**	experiment
$FeC_{34}H_{32}N_4O_4$ (**1**) → $FeC_{32}H_{29}N_4O_2$ (**2**) + H_2CCOOH − $D_1°$	2.72	2.97	2.97	
	(2.45)	(2.70)	(2.70)	
$FeC_{32}H_{29}N_4O_2$ (**2**) → $FeC_{30}H_{26}N_4$ (**3**) + H_2CCOOH − $D_2°$	2.82	2.87	2.67	
	(2.64)	(2.69)	(2.49)	
$FeC_{34}H_{32}N_4O_4^+$ (**1**) → $FeC_{32}H_{29}N_4O_2^+$ (**2**) + H_2CCOOH − D_1^+	2.38	1.94	1.98	$\leq 2.5 \pm 0.3$[4] 1.9 ± 0.2[5]
	(2.20)	(1.76)	(1.80)	
$FeC_{32}H_{29}N_4O_2^+$ (**2**) → $FeC_{30}H_{26}N_4^+$ (**3**) + H_2CCOOH − D_2^+	2.55	2.71	2.65	$\ll D_1$[4]
	(2.31)	(2.47)	(2.41)	2.4 ± 0.3[5]

(b) Elimination of Methyl and Vinyl Groups

reaction	Gen-1	6-31G*	6-311++G**
$FeC_{30}H_{26}N_4^+$ (**3**) → $FeC_{29}H_{23}N_4^+$ (**4**-*1*) − D_1^+(Me)	5.05	4.94	4.47
	(4.75)	(4.64)	(4.17)
$FeC_{29}H_{23}N_4^+$ (**4**-*1*) → $FeC_{28}H_{20}N_4^+$ (**5**) − D_2^+(Me)	4.97	4.74	4.93
	(4.69)	(4.46)	(4.65)
$FeC_{28}H_{20}N_4^+$ (**5**) → $FeC_{27}H_{17}N_4^+$ (**6**) − D_3^+(Me)	4.79	5.13	4.66
	(4.53)	(4.87)	(4.40)
$FeC_{27}H_{17}N_4^+$ (**6**) → $FeC_{26}H_{14}N_4^+$ (**7**) − D_4^+(Me)	4.93	4.92	4.79
	(4.64)	(4.63)	(4.50)
$FeC_{26}H_{14}N_4^+$ (**7**) → $FeC_{24}H_{11}N_4^+$ (**8**) − D_1^+(Vi)	5.34	5.58	5.44
	(5.07)	(5.31)	(5.17)
$FeC_{24}H_{11}N_4^+$ (**8**) → $FeC_{22}H_8N_4^+$ (**9**) − D_2^+(Vi)	5.64		4. 96
	(5.39)		(4.74)

[a] Calculated at the geometry optimized at the B3LYP/Gen-1 level. The D_i values, which were calculated with ZPE(B3LYP/Gen-1) taken into account, are given in parentheses.

to several electronic states with the same total spin but with a different distribution of unpaired electrons between the d-AO's of the metal, between MO's of the P ring, and between the metal and the ring. An in-depth analysis of all of these states is beyond the scope of the present paper, and here, we limited ourselves by optimization of several tens of the most probable structures of high- and middle-spin electronic states and by selection of the most energetically favorable between them. It was emphasized above that the geometry optimization for all structures **4**−**9** was performed without imposing symmetry constraints and that the use of different initial vectors led, as a rule, to the same results. We can hope that the data in Tables 1 and 2 correspond

to the lowest electronic states (or those lying close to the lowest states within an uncertainty of few tenths of an electronvolt) for each structure and multiplicity under consideration (see ref 18 for more detail).

Elimination of one Me group from different meso-positions of the P ring of hemin$^+$ (on the structure **1**, Figure 1, these positions are denoted by latinic figures *1*, *3*, *5*, and *8*) produces four positional isomers of $FeC_{29}H_{23}N_4^+$ with the structures **4**-*1*, **4**-*3*, **4**-*5*, and **4**-*8*. The first three isomers have the lowest triplet state, and among these three, the triplet **4**-*1*, in which the Me group is deleted from the meso-atom C_{21}, is the most favorable (in Table 1, these types of multiplets, which are most favorable in energy among the states of the same multiplicity and in which the spin density on the Fe atom is denoted by index *a*). The triplets of the rest isomers lie higher by a few tenths an electronvolt. The computational results for all positional isomers are similar in many aspects, and here, we focus on the favorable isomer **4**-*1* with various multiplicities.

In the triplet **4**-*1*(1-*a*), the Fe atom has two unpaired electrons (ρ(Fe) $\sim$ 2.00), and the spin density of the P ring is polarized significantly. One spin of the ring, which is parallel to the spins of the metal, is localized at the "radical" atom C_{21} ($\rho(C_{21}) \sim$ 1.03), and the second (antiparallel) spin is "smeared" over the ring (mostly on C_{15}, C_{19}, C_{28}, C_{29}, and the nitrogen atoms). In the quintet **4**-*1*(2-*a*), both the Fe atom and the P ring possess two spins each. Like in the triplet, one spin of the ring is localized at the radical center C_{21}, and the second spin is spread over the ring. At the triplet−quintet excitation, the spin state of Fe does not change, but the antiparallel spins of the ring are reoriented to be parallel with each other and with the spins of the metal. In the septet **4**-*1*(3-*a*), the Fe atom and P ring have four and two parallel spins, respectively.

For the isomer **4**-*3*, in addition to the lowest quintet *a*, another higher-lying (by $\sim$1.1 eV) quintet *b* was localized, in which most of spin density was distributed over the ring. In contrast to the septet **4**-*1*(3-*a*), the septets of the isomers **4**-*3*, **4**-*5*, and **4**-*8* are much less favorable as compared with those of the triplets; their spin density is shared almost evenly between the metal and the ring (in Table 1, they are denoted as 3-*c*). Our attempts to localize the lowest (of the *a* type) septets for the **4**-*3*, **4**-*5*, and **4**-*8* isomers and the lowest triplet for **4**-*8* failed due the convergency problems. Instead, for **4**-*8*, another high-lying triplet 1-*d* was localized with a different (as compared with 1-*a*) spin-density distribution.[18]

Ion $FeC_{28}H_{20}N_4^+$ (**5**) has six low-lying positional isomers. Their computational results are also quite similar, and we will focus on the lowest-energy isomer **5**-*1*(*3*), for which the quartet, sextet, and octet lie close to each other within 0.15 eV. In the slightly preferable sextet, the Fe atom has two (ρ(Fe) $\sim$ 1.97), and the P ring has three unpaired electrons. Two from the latter three are localized at the radical centers C_{21} and C_{24} ($\rho(C_{21})-\rho(C_{24}) \sim$ 1.0), and the third spin is delocalized mostly between the same C_{15}, C_{19}, C_{28}, and C_{29} atoms as those in the triplet **4**-*1* (see above). At the sextet−quartet transition, the spin state of Fe changes slightly, but the spins of the ring are reoriented. In contrast, at the sextet−octet excitation, the spin state of the ring changes marginally, but the Fe atom is promoted from the middle-spin to the high-spin state (ρ(Fe) $\sim$ 3.76 in the octet), in accord with shortening of the *R*(FeN) distance in the quartet and sextet and its elongation in the septet.[18]

For the $FeC_{27}H_{17}N_4^+$ (**6**) ion with three missing Me groups, the septet is favorable, in which about three unpaired electrons are localized on the Fe atom and another three on the radical centers C_{21}, C_{24}, and C_{15} of the ring. The quintet and triplet lie higher by $\sim$0.5 and 1.2 eV. At last, for the $FeC_{26}H_{14}N_4^+$ (**7**) ion (with all four Me groups missing), the octet is preferable, with three spins on the metal and four spins on the radical meso-centers C_{21}, C_{24}, C_{15}, and C_{19}.

For the $FeC_{24}H_{11}N_4^+$ (**8**) ion, in which only one vinyl group is preserved, the high-spin states with $M = 7$ and 9 are the most profitable, and for the "naked" $FeC_{22}H_8N_4^+$ (**9**) ion, the lowest quartet, sextet and octet, are quasi-degenerated in energy. In the latter two, Fe has two unpaired electrons, and the rest spin density is mostly localized at the radical C atoms and partially spread over the all-P skeleton with different signs on different atoms.

One can see that, at the B3LYP/6-311++G**//B3LYP/Gen-1 + ZPE(B3LYP/Gen-1) level, upon the stepwise elimination of each peripheral Me or Vi group from heme and hemin$^+$, one spin is retained localized on the "radical" atom C, which was directly bonded with this group. Polyradical character of the P ring is enhanced with an increase of the number of the eliminated groups. The states of the lower multiplicity, in which the ring spins are coupled (or decoupled) and are directed in parallel (or antiparallel) with the spins of the metal, can approach or even lie close in energy to the high-spin states. As the first approximation, the metal atom and the "naked" P ring can be treated as a system of the coupled reservoirs of unpaired electrons with variable capacity. Different mutual orientations of spins can be manifested in antiferromagnetic couplings between the metal and the ring and are anomalous and different for different state dependences of magnetic properties from temperature.

Certainly, our discussion of the unpaired electron distribution, which is based on the spin density data ρ, calculated in the framework of the Mulliken population analysis, is approximate. It should be emphasized however that the calculated ρ values appear to be only slightly sensitive to the basis set used; therefore, one can believe that the conclusions based on integer (or nearly integer) ρ(Fe) values can be treated as reliable. It is more challenging to interpret ρ for low-spin states where the correct wave function should include several determinants; nevertheless, it is hoped that the corresponding corrections do not change the semiquantitative pattern.

Geometric parameters of the P skeleton and the peripheral groups are rather moderately (mostly within 0.01−0.02 Å and few degrees) varied in the series under discussion.[5,13,18] One can note a perceivable enhancement of the bond alternation at the periphery and inside of the P ring with a decreasing number of eliminated external groups. The strongest elongation (by 0.05−0.07 Å) is observed for the "outer" pyrrole bonds like $C_{15}-C_{16}$ and $C_{18}-C_{19}$. Lengths of the bonds both in the peripheral groups and between them and the P skeleton are the least sensitive to charge and multiplicity. The changes in their lengths rarely exceed 0.01 Å. The Fe atom in all of the structures and states under consideration remains in the plane NNNN of the four nitrogen atoms and is located in (or almost in) its center.

Calculated energies D_i^+(Me) of consecutive elimination of the methyl groups from the $FeC_{30}H_{26}N_4^+$ (**3**) ion (Table 2b) lie within the range of 4.2−4.6 eV and are almost twofold larger as compared with the energies D_i(CMe) and D_i^+(CMe) of cleavage of the carboxymethyl groups from heme and hemin$^+$ (Table 2a). This result is related to the fact than when a carboxymethyl group is removed, the $C_{16}-C_{28}$ and $C_{18}-C_{29}$ single bonds, which link these CMe groups to the porphyrin skeleton, become double bonds, which follows from the significant increase in their overlap populations and the decrease in their bond lengths from 1.50 in hemin$^+$ (**1**) to 1.35−1.38 Å

TABLE 3: Relative Energies of Multiplets, Effective Charges, and Spin Densities on Fe Atoms in the Ferriporphyrin Dimer Molecule and Ion and in Products of Their Degradation[a]

species	spin S	E_{rel}[b] eV	Z(Fe) e	ρ(Fe) e
$(FeC_{34}H_{31}N_4O_4)_2$	5	∼0.	+1.34, +1.34	4.29, 4.29
	4	0.0	+1.34, +1.29	4.29, 2.84
	3	∼0.	+1.23, +1.23	2.84, 2.84
	2	0.38	+1.23, +1.19	2.84, 1.16
	1	0.38	+1.22, +1.18	2.77, −1.08
	0	3.32	+1.15, +1.15	
$(FeC_{34}H_{31}N_4O_4)_2^+$	$4^1/_2$	0.49	+1.35, +1.24	4.29, 2.83
	$3^1/_2$	0.	+1.25, +1.24	2.87, 2.82
	$2^1/_2$	0.	+1.24, +1.19	2.83, 1.06
	$1^1/_2$	0.62	+1.24, +1.20	2.81, 1.02
	$^1/_2$	1.20	+1.22, +1.19	1.02, 0.83

species	spin	E_{rel}[b]	Z(Fe) Z(O*)[c]	ρ(Fe) ρ(O*)[c]
$FeC_{34}H_{31}N_4O_4$	$2^1/_2$	0.21	+1.08 −0.36	3.81 0.50
	$1^1/_2$	0.	+1.16 −0.41	2.67 0.33
	$^1/_2$	0.47	+0.93 −0.22	∼0 ∼0.86
$FeC_{34}H_{31}N_4O_4^+$	2	0.0	+1.27 −0.22	2.95 0.85
	1	0.0	+1.27 −0.22	2.94 −0.86
	0	2.25	+1.06 −0.36	

[a] Calculated at the B3LYP/Gen-2//B3LYP/Gen-1 level. In the Z(Fe) and ρ(Fe) columns, the first values refer to the Fe atom with the largest number of unpaired electrons. [b] Calculated with respect to the ground state. [c] The bridged (directly bonded with Fe) oxygen atom O* of the dehydrogenated carboxyl group (see Figure 4).

TABLE 4: Energies of Dissociation of the Ferriporphyrin Dimer and Its Ion into the Monomers and Their Ionization Potentials, Calculated at the B3LYP Level Using the Gen-1 and Gen-2 Basis Sets[a] (in eV)

reaction	Gen-1	Gen-2
$(FeC_{34}H_{31}N_4O_4)_2 \rightarrow 2FeC_{34}H_{31}N_4O_4 - D°$	3.30	3.34
$(FeC_{34}H_{31}N_4O_4)_2^+ \rightarrow FeC_{34}H_{31}N_4O_4 + FeC_{34}H_{31}N_4O_4^+ - D^+$	3.65	3.75
$(FeC_{34}H_{31}N_4O_4)_2 \rightarrow (FeC_{34}H_{31}N_4O_4)_2^+ - IP_{dim}$	6.21	5.82
$FeC_{34}H_{31}N_4O_4 \rightarrow FeC_{34}H_{31}N_4O_4^+ - IP_{mon}$	6.25	6.30

[a] At the geometry optimized at the B3LYP/Gen-1 level.

in $C_{32}H_{29}O_2N_4^+$ (**2**) and $FeC_{30}H_{26}N_4^+$ (**3**). The energy expenditure for detachment of the first and the second CMe groups is partially (and significantly) compensated by the formation of the π bonds $C_{16}-C_{28}$ and $C_{18}-C_{29}$. In this context, the statement[4] that D_2^+(CMe) is much smaller than D_1^+(CMe) seems to be debatable.

The energy D_1^+(Vi) of abstraction of the first vinyl group is by ∼0.5 eV larger as compared with the second one D_2^+(Vi) and by ∼1.0 eV larger than D_1^+(Me) (Tables 2 and 4). As much as the calculated elimination energies D_1^+(CMe) and D_2^+(CMe) for the carboxymethyl groups are in good agreement with the experimental data,[5] one can believe that an error of the calculated bond dissociation energies for other external groups does not significantly exceed a few tenths of an electronvolt.[18] Increasing of the energy D_i^+ in the series CMe ≪ Me < Vi corresponds well to the experimental finding that the carboxymethyl groups are first and most readily removed; the methyls are the next, and the vinyl groups are the last to be eliminated in this series.

IV. Dimer of Ferriporphyrin $(FeC_{34}H_{31}N_4O_4)_2$ and Its Ion $(FeC_{34}H_{31}N_4O_4)_2^+$

Synthetic β-hematin is chemically, spectroscopically, and crystallographically identical to natural hemozoin (malarial pigment). It is composed of polymeric chains consisting of Fe(III) porphyrin units linked by Fe propionate oxygen bridge bonds. The structure of powdery β-hematin, determined by X-ray diffraction,[19] is characterized by a triclinic unit cell. Its lattice is built up of ferriporphyrin dimers $(FeC_{34}H_{31}N_4O_4)_2$ (a local symmetry of C_i), and each of the dimers is linked with the two neighboring blocks by hydrogen bridges between "free" propionate groups. ESR and Mössbauer studies of bulk β-hematin and malarial pigment indicate that the iron atoms in them are in the high-spin state and each has five unpaired electrons.[20] Knowledge of the structures of these compounds will shed light on the mechanisms of the action of antimalarial drugs.[19]

Geometric parameters of the ferriporphyrin dimer, optimized at the B3LYP/Gen-1 level (see Figure 4), are collected in ref 21. Its optimized best structure is depicted in Figure 4. As seen in Table 3, for the neutral $(FeC_{34}H_{31}N_4O_4)_2$ molecule, a group of three close-lying electronic states with the multiplicities $M = 11$, 9, and 7 is most favorable. According to the calculated ρ(Fe) values, in the states with $M = 11$ and 7, each Fe atom has five and three unpaired electrons, respectively, while in the state with intermediate $M = 9$, one Fe atom has five and the second one has three unpaired electrons. The calculation results for the isolated molecule $(FeC_{34}H_{31}O_4N_4)_2$ and the experimental data of ESR and Mössbauer spectra for bulk β-hematin and malaria pigment[20] agree that the ground state has the high spin in the both cases, but the calculations predict also that the high-spin state $M = 11$ is close in energy with the other two multiplets $M = 9$ and 7.

For the $(FeC_{34}H_{31}O_4N_4)_2^+$ dimer ion, the quasi-degenerate octet and sextet are preferable. In the octet, both Fe atoms have three unpaired electrons each, and one additional spin is symmetrically delocalized among the rings, mostly on the bridging oxygen atoms O* and on the carbon atoms nearest to the iron atoms. The electronic state with $M = 10$, where one Fe atom has four and another one has three unpaired electrons, lies ∼0.5 eV higher. The quartet and doublet states are even less favorable by an additional ∼0.12 and ∼0.7 eV. The energy $D°$ of dissociation of the neutral dimer to two monomers calculated for their lowest multiplets is ∼3.34 eV (Table 4), while the dissociation energy D^+ for the dimer ion is 0.4 eV higher at 3.75 eV. The calculations with both basis sets, Gen-1 and Gen-2, give similar results.

As it was found in ref 21, the calculated (for the isolated $(FeC_{34}H_{31}O_4N_4)_2$ molecule) and experimental (for the bulk β-hematin) bond lengths in the P rings in the high-spin ($M = 11$) state generally agree well with each other. The differences do not exceed the conventional computational inaccuracy of ∼0.01−0.02 Å and a few degrees, with the exception of the external bonds like C_7-C_{15} in pyrrol cycles, for which the calculated values are 0.027 Å longer than the experimental data. In addition, in β-hematin, the bond alternation in the P rings is somewhat more pronounced than that in the isolated dimer. The computed distances R(Fe−N), displacement h(Fe) of the Fe atom perpendicular to the NNNN plane, the φ(NFeN) bond angle, and the R(Fe−O) bond length coincide with their experimental values within the same range of ∼0.02 Å and ∼1°.

For the peripheral groups, the discrepancies are more significant, especially for their orientation with respect to the P ring and the corresponding torsion angles. As was emphasized earlier,[21] some experimental data given in the attachment[19] seem arguable. For instance, for the double C=C bonds of the planar vinyl groups, the values of 1.26(4) and 1.31(4) Å are specified in ref 19, among which the former is rather close to a conventional triple bond length, while our calculation results in the same value of 1.34 Å for both groups.[21] The lengths of ordinary C−C bonds that connect methyl groups with the P

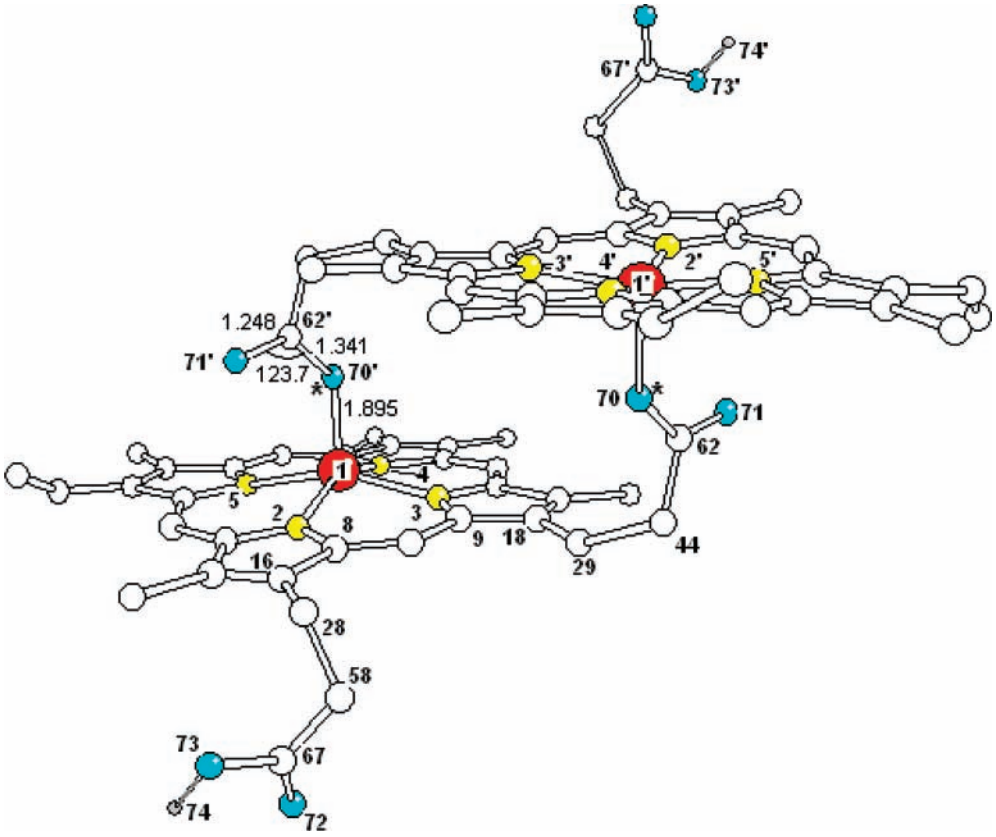

Figure 4. The structure of the ferriporphyrin dimer $[Fe(III)C_{34}H_{31}O_4N_4]_2$ ($M = 11$) and its positive ion. The hydrogen atoms are omitted.

ring given in the ref 19 vary from 1.50 to 1.57 Å, whereas our calculations assign nearly the same value of 1.50 Å for all four Me groups.[21] The reasons for such strong differences in the bond lengths and bond angles of chemically equivalent external groups (significant contraction of the double bonds in the vinyl group and elongation of the single bonds between methyl groups and the P ring) remain unclear. The magnitude of the angle φ(OCO*) = 110.8° given in the ref 19 seems to be underestimated (our calculation provides 122°) because this angle in carboxy compounds usually exceeds the value of 120°, corresponding to sp^2-hybridization, owing to a repulsion of negatively charge oxygen atoms.

Due to the "$3d_{x^2-y^2}$ Fe AO effect", in the high-spin state of the neutral $(FeC_{34}H_{31}O_4N_4)_2$ with $M = 11$, the distance R(Fe−N) is ∼0.07 Å longer, R(Fe−O*) is ∼0.05 Å shorter, the out-of-plane displacement of the metal h(Fe) is ∼0.17 Å, and the angle φ(NFeN) is ∼2° smaller than those in the heptet state in which the $d_{x^2-y^2}$ AO remains vacant and can participate in the formation of donor−acceptor bonding with the lone pairs of the N atoms. Similarly, in the neutral dimer with the intermediate multiplicity $M = 9$ and in the ion with $M = 10$ in the ring, which contains the high-spin Fe atom, the distance R(Fe−N) is 0.06−0.07 Å longer, R(Fe−O*) is 0.03−0.05 Å shorter, h(Fe) is 0.10−0.17 Å larger, and φ (NFeN) is 1−2° less than those in the second ring with the intermediate-spin Fe atom.

Certainly, the comparison of the equilibrium geometry of the isolated dimer molecule $(FeC_{34}H_{31}O_4N_4)_2$ with the "effective" experimental geometry of powder β-hematin is approximate. Deviations between the two geometries can be caused, on one hand, by inaccuracies of the calculations both in the B3LYP approximation and in the mathematical treatment of the X-ray results; the latter can be especially pronounced in nonrigid crystals of low symmetry with light atoms in combination with heavy atoms like Fe. On the other hand, discrepancies can result from various "bulk" effects (packing effects, reorientation of the propionate groups which form the hydrogen bonds with the neighboring dimers, interactions between P rings of neighboring blocks, the temperature factor, etc.), which are considerable in condensed matter but absent or minor in an isolated molecule. For that reason, we focused mostly on parameters of the P rings and on the bridge bonds between the rings, where these "bulk" effects should be minimal and where agreement between calculations and experiment was satisfactory. Nevertheless, the above-mentioned strong deviations for the peripheral groups, which much exceed the conventional computational errors of the B3LYP approximation, point out that the structure of both the isolated $(FeC_{34}H_{31}O_4N_4)_2$ molecule and bulk β-hematin need to be refined.

V. Heme Dimer $(FeC_{34}H_{32}N_4O_4)_2$ and Its Ion $(FeC_{34}H_{32}N_4O_4)_2^+$

The positive heme dimer ion $(FeC_{34}H_{32}N_4O_4)_2^+$ was observed in a study of the heme complex with myoglobin[22] using electrospray mass spectrometry, laser excitation, and the CID method, but to our knowledge, its electronic, geometric, and energetic properties are not known.

The lowest optimized (at the B3LYP/Gen-1 level) structure of the $(FeC_{34}H_{32}N_4O_4)_2^+$ ion[23] is depicted in Figure 5, and its energetic and some equilibrium geometric parameters are given in Tables 5 and 6 and Figure 5. One can see from Figure 5 and Table 6 that the bonding between two P rings is formed by a pair of Fe−carboxyl (Fe···O*═C(OH)) and a pair of hydrogen (OH_b···N) bonds. It should be noted that two local minima, very close (within ∼1 kcal/mol) in energy, have been localized on the PES of the $(FeC_{34}H_{32}N_4O_4)_2^+$ ion.[23] One of them corresponds to the center-symmetrical structure (C_i), similar to that of the ferriporphyrin dimer. The second, more favorable

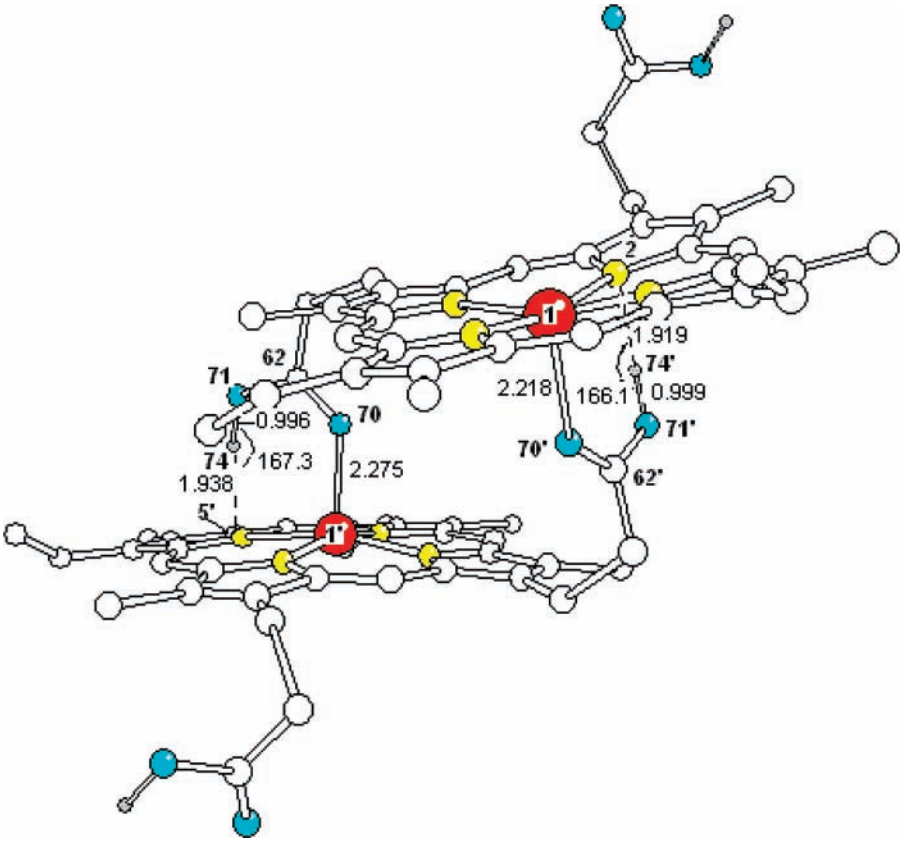

Figure 5. The structure of the dimer $(heme)_2^+$ ion ($M = 6$).

TABLE 5: Relative Energies of Low-Lying Multiplets, Effective Charges, and Spin Densities on Fe Atoms in the $(Heme)_2$ Dimer Molecule and Its Cation $(Heme)_2^+$[a]

species	spin S	E_{rel}[b] eV	Z(Fe) e	ρ(Fe) e
$(FeC_{34}H_{32}N_4O_4)_2$	4	0.10	+1.14, +1.14	3.91, 3.91
	3	0.12	+1.12, +1.05	3.81, 2.13
	2	0.	+1.03, +1.03	2.17, 2.17
$(FeC_{34}H_{32}N_4O_4)_2^+$	$4^1/_2$	0.19	+1.27, +1.27	4.14, 4.14
	$3^1/_2$	0.15	+1.20, +1.18	3.54, 3.35
	$2^1/_2$	0.	+1.18, +1.16	2.65, 2.55
	$1^1/_2$	0.52	+1.25, +1.06	2.92, ~0

[a] Calculated at the B3LYP/Gen-2//B3LYP/Gen-1 level. In the Z(Fe) and ρ(Fe) columns, the first values refer to the Fe atom with the largest number of unpaired electrons. [b]With respect to the most preferable state.

TABLE 6: Energies of Dissociation of $(Heme)_2$ and $(Heme)_2^+$ Dimers into the Monomers Calculated at the B3LYP Level with Using Gen-1 and Gen-2 Basis Sets (in eV)[a]

reaction	Gen-1	Gen-2
$(FeC_{34}H_{32}N_4O_4)_2 \rightarrow 2FeC_{34}H_{32}N_4O_4 - D°$	0.10	0.30
$(FeC_{34}H_{32}N_4O_4)_2^+ \rightarrow FeC_{34}H_{32}N_4O_4 + FeC_{34}H_{32}N_4O_4^+ - D^+$	1.01	1.40

[a] At the geometry optimized at the B3LYP/Gen-1 level.

nonsymmetrical minimum (C_1) is related to another structure, the rings of which are tilted and rotated relative to each other by angles of ~15−20°. The latter, depicted on Figure 5, possesses better steric conditions for enhancing the hydrogen bonds and will be discussed below.

For the $(heme)_2^+$ ion, three close-lying (within 0.2−0.3 eV) states with $M = 10$, 8, and 6 are favorable (Table 5). The first state, with the highest spin each Fe atom, has four unpaired electrons ($\rho(Fe_1)-\rho(Fe_2) \sim 4.14$), and one spin is spread over both rings (mostly on the nitrogen atoms). In the octet and in the sextet, all seven and all five spins, respectively, are localized at the Fe atoms ($\rho(Fe_1) \sim 3.5$ and $\rho(Fe_2) \sim 3.35$ for $M = 8$; $\rho(Fe_1) \sim 2.65$ and $\rho(Fe_2) \sim 2.55$ for $M = 6$). The sextet is most preferable. In the higher-lying and especially in the low-spin states, the ρ distribution can be asymmetrical, with a different number of spins for different Fe atoms ("spin disproportion"). One can suppose that the low-lying excited electronic states of the $(heme)_2^+$ ion with different multiplicities, structures, and ρ distributions can be easily promoted at a quite modest or small change in energy.

From Table 6, one can see that the sextet $(heme)_2^+$ should be rather stable. Its energy of dissociation D^+ into the ground multiplets of the monomer heme (triplet) + hemin$^+$ (quartet), computed at the B3LYP/Gen-2 level, is about 1.4 eV, in agreement with high intensity of this ion in the mass spectra[22] and with the rather short distances of R(Fe···O*) ~ 2.2 Å and $R(H_b\cdots N) \sim 1.9$ Å in the both pairs of the oxygen and hydrogen bridges connecting the P rings.

In contrast to hemin$^+$, which has the planar "core" Fe@N_4, in the $(heme)_2^+$ dimer, both Fe atoms are shifted perpendicular to their NNNN planes, and the P rings undergo a significant dome deformation. Again, due to the "$3d_{x^2-y^2}$ Fe AO effect", in the ring with Fe in the high-spin state, R(Fe−N) is longer, R(Fe−O*) is shorter, the shift h(Fe/NNNN) is ~0.17 Å larger, and φ (NFeN) is ~2° less than those in the ring with the metal in the middle- or low-spin state.

The neutral heme dimer also has three low-lying multiplets with $M = 9$, 7, and 5. The quintet is preferable (Table 5). In the states with $M = 9$ and 5, both Fe atoms are almost equivalent and, respectively, have four and two unpaired electrons each. In the "intermediate" heptet, one Fe has four and the other Fe

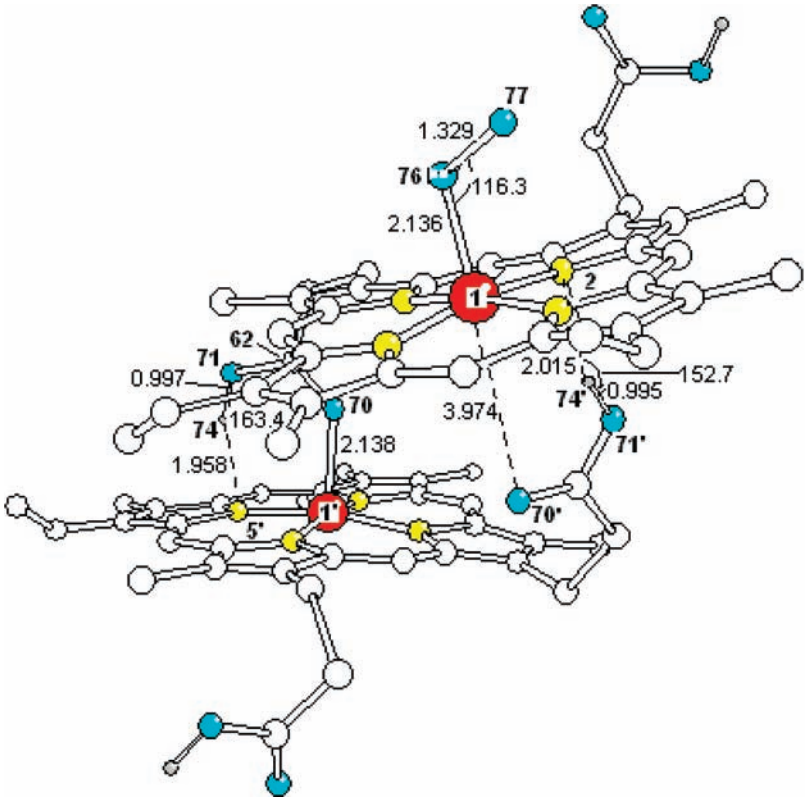

Figure 6. The structure of the dimer $(heme)_2^+O_2$ ($M = 8$) complex ion.

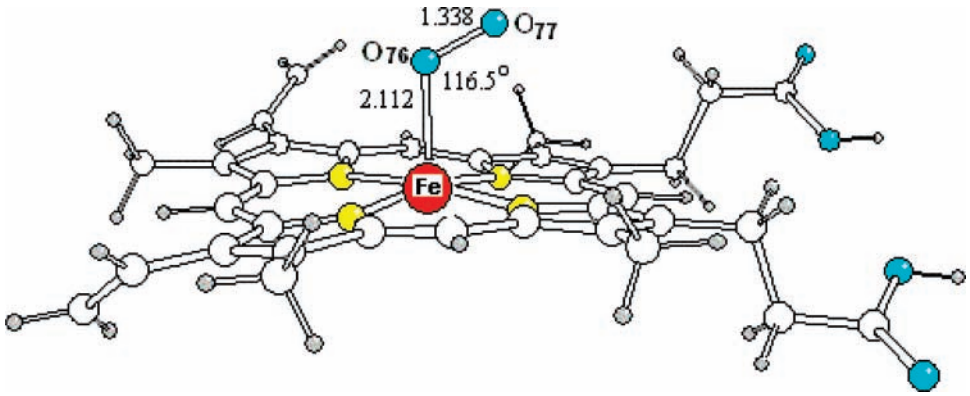

Figure 7. Structure of the monomer $hemeO_2$ ($M = 5$) complex.

has two spins, and the P rings differ from each another both by the ρ distribution and by geometry (especially by torsion angles[23]).

The most significant difference between the neutral $(heme)_2$ dimer and its ion $(heme)_2^+$ is the quite low stability of the former. The calculated dissociation energy D^0 for $(heme)_2$ (quintet) $\rightarrow$ 2 heme (triplet) is only tenths of an electronvolt, and distances R(Fe···O*) in the $(heme)_2$ (quintet) is 0.2−0.4 Å longer than that in the $(heme)_2^+$ ion. In accord with the calculations, the neutral $(heme)_2$ dimer should be treated as a weakly bonded molecular complex.

VI. Interaction of Dimers $(Heme)_2$, $(Heme)_2^+$, and $(Ferriporphyrin)_2$ with Molecule O_2

Our similar B3LYP calculations of the PES and geometry optimization of the neutral and cationic dioxygenyl complexes $(heme)_2O_2$, $(heme)_2^+O_2$, and $(ferriporphyrin)_2O_2$ in the high-spin states and in the vicinity of the structures, in which the axial oxygen molecule occupies a fifth coordinational position above one of the Fe atoms, produced the following results.[23,24] The weakly bonded neutral heme dimer appeared to be practically unstable toward the barrierless dissociation into two monomeric products, the complex $hemeO_2$ + heme. For $(ferriporphyrin)_2O_2$ we could not locate a binding structure at all. Its PES was found to be of repulsive character, and upon optimization, the $(ferriporphyrin)_2$ dimer and the O_2 molecule were separated from each other by a distance more than 5 Å. In other words, at the B3LYP/Gen-1 level, the $(ferriporphyrin)_2$ dimer molecule does not possess an affinity to molecular oxygen, and the neutral $(heme)_2O_2$ dimer easily splits into the heme monomer and the five-coordinated $hemeO_2$. The cationic $(heme)_2^+O_2$ complex in the most favorable octet state (depicted in Figure 6), in contrast to the two former complexes, was found to be stable toward the abstraction of the O_2 molecule and even more stable toward the dissociation into the monomers $hemin^+O_2$ + heme or $hemeO_2$ + $hemin^+$. The structure of $(heme)_2^+O_2$

can be approximately interpreted as that of an associate of the heme dioxygenyl with hemin$^+$, in which only one bonding oxygen bridge Fe···O*═C(OH) with the noncoordinated $Fe_{1'}$ atom and one neighboring hydrogen bond HO···N (in the left half of Figure 6) are preserved. In the right half of Figure 6, the second oxygen bridge with the Fe_1 atom, which is coordinated to the O_2 molecule, is broken completely, and the H bond is weakened significantly; the distance $R(N_2-H_{74'})$ elongates to 2.015 Å, $R(O_{71'}-H_{74'})$ shortens to 0.995 Å, and $\varphi(O_{71'}H_{74'}N_2)$ decreases to 152.7° against the corresponding values of 1.919 Å, 0.999 Å, and 166.1° in the free $(heme)_2^+$ dimer (with $M = 6$). The coordinated Fe_1 atom is shifted from the NNNN plane in a direction toward the axial O_2 molecule by ~0.16 Å and forms a stronger Fe_1-OO bond. The calculated distances $R(Fe_1-OO) = 2.136$ and $R(O_{76}-O_{77}) = 1.329$ Å and the angle $\varphi(Fe_1OO) = 116.3°$ in the dimer $(heme)_2^+O_2$ complex are close to the corresponding values of 2.111 Å, 1.333 Å, and 116.5° in the monomer $hemeO_2$ complex optimized by us within the same B3LYP/Gen-1 approximation (the equilibrium structure of $hemeO_2$ ($M = 5$) is depicted on Figure 7). The elongated $R(O-O)$ distance ~1.329 Å and the pattern of ρ distribution indicate that the axial O_2 ligand in $(heme)_2^+O_2$ is coordinated to the Fe_1 atom as a superoxide anion O_2^- with significant charge transfer from the ligand to the metal.

Calculated energies of $(heme)_2^+O_2$ ($M = 8$) dissociation into $(heme)_2^+$ ($M = 8$) + O_2 ($M = 3$) with loss of molecular oxygen, on one hand, and into the monomers $hemin^+O_2$ + heme or $hemeO_2$ + hemin$^+$, on the other hand, are ~0.25 and ~0.90 kcal/mol (the products of the latter two channels of decay are very close in energy). Surely, these values are approximate (among other factors, zero-point energies were not taken into account), but they indicate, at the semiquantitative level, that in contrast to the ferriporhyrine dimer, the $(heme)_2^+$ dimer ion can form a rather stable complex with O_2.

In conclusion, it should be emphasized that practically all of the systems under consideration in the present paper have very flat potential energy surfaces and 10 or more vibrational frequencies in the least-long wavelength range from 10 to 20 to 100 cm^{-1}, which correspond to the out-of-plane distortions of the P ring and to rotations of peripheral groups about single bonds. It is evident that, at common temperatures, many or most of these low-lying vibrational levels should be populated, and the effective structure, which is obtained by averaging over all populated levels, can differ (maybe considerably) from the equilibrium structure. The static geometry concept is not fully adequate in this case, and nonempirical dynamic approaches should be used for describing the ring conformations and mutual orientations of the peripheral groups with respect to the P rings.

In our following papers, other compounds of heme and hemin$^+$ with atomic and molecular oxygen and with CO, NO, CN^-, OOH, and related ligands will be discussed.

Acknowledgment. The authors thank the Computer Center of Academia Sinica and the National Center for High-Performance Computations of Taiwan for computer time and help in performing calculations. O.P.C. and N.M.K. thank Professor S. H. Lin for the invitation to visit the Institute of Atomic and Molecular Science, Academia Sinica in Taipei and for financial support.

References and Notes

(1) *The Porphyrine Handbook*; Kadish, K. M., Smith, K. M., Gillard, R. Eds.; Academic Press: San Diego, CA, 2000.

(2) Kalyanasundaram, K. *Photochemistry of Polypyridine and Porphyrine Complexes*; Academic Press: London, 1992.

(3) *Electrospray Ionization Mass-Spectrometry*; Cole, R. B., Ed.; Wiley: New York, 1997.

(4) Nonose, S.; Tanaka, H.; Okai, N.; Shibakusa, T.; Fuke, K. *Eur. Phys. J.* **2002**, *D20*, 619.

(5) Charkin, O. P.; Klimenko, N. M.; Charkin, D. O.; Nguyen, T. P.; Wang, Y.-S.; Wei, S.-C.; Lin, S. H.; Chang, H.-C. *Chem. Phys. Lett.* **2005**, *415*, 362.

(6) Rivera, M.; Caignan, G. A.; Astashkin, A. V.; Raitsimring, A. M.; Shokhivera, T. K.; Walker, F. A. *J. Am. Chem. Soc.* **2002**, *124*, 6077.

(7) Shaik, S.; Filatov, M.; Schroeder, D.; Schwartz, H. *Chem.—Eur. J.* **1998**, *4*, 193.

(8) Becke, A. D. *J. Chem. Phys.* **1993**, *98*, 5648.

(9) Lee, C.; Yang, W.; Parr, R. G. *Phys. Rev. B* **1988**, *37*, 785.

(10) Frisch, M. J.; Trucks, G. W.; Schlegel, H. B.; Scuseria, G. E.; Robb, M. A.; Cheeseman, J. R.; Montgomery, J. A., Jr.; Vreven, T.; Kudin, K. N.; Burant, J. C.; Millam, J. M.; Iyengar, S. S.; Tomasi, J.; Barone, V.; Mennucci, B.; Cossi, M.; Scalmani, G.; Rega, N.; Petersson, G. A.; Nakatsuji, H.; Hada, M.; Ehara, M.; Toyota, K.; Fukuda, R.; Hasegawa, J.; Ishida, M.; Nakajima, T.; Honda, Y.; Kitao, O.; Nakai, H.; Klene, M.; Li, X.; Knox, J. E.; Hratchian, H. P.; Cross, J. B.; Bakken, V.; Adamo, C.; Jaramillo, J.; Gomperts, R.; Stratmann, R. E.; Yazyev, O.; Austin, A. J.; Cammi, R.; Pomelli, C.; Ochterski, J. W.; Ayala, P. Y.; Morokuma, K.; Voth, G. A.; Salvador, P.; Dannenberg, J. J.; Zakrzewski, V. G.; Dapprich, S.; Daniels, A. D.; Strain, M. C.; Farkas, O.; Malick, D. K.; Rabuck, A. D.; Raghavachari, K.; Foresman, J. B.; Ortiz, J. V.; Cui, Q.; Baboul, A. G.; Clifford, S.; Cioslowski, J.; Stefanov, B. B.; Liu, G.; Liashenko, A.; Piskorz, P.; Komaromi, I.; Martin, R. L.; Fox, D. J.; Keith, T.; Al-Laham, M. A.; Peng, C. Y.; Nanayakkara, A.; Challacombe, M.; Gill, P. M. W.; Johnson, B.; Chen, W.; Wong, M. W.; Gonzalez, C.; Pople, J. A. *Gaussian 03*, revision B.03; Gaussian, Inc.: Pittsburgh, PA, 2004.

(11) Gosh, A. In *The Porphyrin Handbook*; Kadish, K. M., Smith, K. M., Guilard, R., Eds.; Academic Press: San Diego, CA, 2000; Chapter 47.

(12) Lecomte, C.; Rohmer, M.-M.; Benard, M. In *The Porphyrin Handbook*; Kadish, K. M., Smith, K. M., Guilard, R., Eds.; Academic Press: San Diego, CA, 2000; Chapter 48.

(13) Charkin, O. P.; Klimenko, N. M.; Charkin, D. O.; Nguyen, T. P.; Mebel, A. M.; Wang, Y.-S.; Chang, H.-C.; Lin, S.-H. *Russ. J. Inorg. Chem.* (*Engl. Transl.*) **2005**, *50*, 50.

(14) (a) Kozlowski, M.; Spiro, T. G.; Berces, A.; Zgierski, M. Z. *J. Phys. Chem. B* **1998**, *102*, 2603. (b) Zigerski, M. Z.; Kozlowski, P. M.; Patchkovskii, S. *J. Chem. Phys.* **2004**, *121*, 1317.

(15) Ugalde, J. M.; Dunitz, B.; Dreuw, A.; Head-Gordon, M.; Boyd, R. J. *J. Phys. Chem. A* **2004**, *108*, 4653.

(16) Collman, J. P.; Hoard, J. L.; Kim, N.; Lang, G.; Reed, C. A. *J. Am. Chem. Soc.* **1975**, *97*, 2676.

(17) Reed, C. A.; Mashiko, T.; Sheidt, W. R.; Spartalian, K.; Lang, G. *J. Am. Chem. Soc.* **1980**, *102*, 2073.

(18) Charkin, O. P.; Klimenko, N. M.; Charkin, D. O.; Nguyen, T. P.; Wang, Y.-S.; Chang, H.-C.; Lin, S.-H. *Russ. J. Inorg. Chem.* (*Engl. Transl.*) **2006**, *51*, 1613.

(19) Pagola, S.; Stephens, P. W.; Bohle, D. S.; Kosar, A. D.; Madsen, S. K. *Nature* **2000**, *404*, 307.

(20) Bohle, D. S.; Debrunner, P.; Jordan, P. A.; Madsen, S. K.; Schulz, C. A. *J. Am. Chem. Soc.* **1998**, *120*, 8255.

(21) Charkin, O. P.; Klimenko, N. M.; Charkin, D. O.; Nguyen, T. P.; Wang, Y.-S.; Chang, H.-C.; Lin, S.-H. *Russ. J. Inorg. Chem.* (*Engl. Transl.*) **2006**, *51*, 89.

(22) Wang, Y.-S.; Chang, H.-C. Unpublished results.

(23) Charkin, O. P.; Klimenko, N. M.; Charkin, D. O.; Lin, S.-H. *Russ. J. Inorg. Chem.* (*Engl. Transl.*) **2007**, *52*, 1088.

(24) Charkin, O. P.; Klimenko, N. M.; Charkin, D. O.; Lin, S.-H. *Russ. J. Inorg. Chem.* (*Engl. Transl.*) **2007**, *53*, in print.